



# OPEN Effects of the mitoxantrone thermosensitive liposome nanodelivery system on prostate cancer in vivo and in vitro

Yuan Gao<sup>1,4</sup>, Tianjiao Wen<sup>2,4</sup>, Bin Shan<sup>2</sup>, Meng Meng<sup>2</sup>, Jing Bai<sup>2</sup>, Wei Tian<sup>3</sup>✉ & Congxin Li<sup>1</sup>✉

This study aimed to prepare mitoxantrone thermosensitive liposome (MTX-TSL) to enhance the targeting capability of liposomes and thus improve the therapeutic effect of the drug on prostate cancer. MTX-TSL were prepared using the thin-film hydration method. A single-factor experiment was conducted to optimize the formulation process, and the liposome quality was assessed alongside short-term stability testing. The *in vitro* efficacy of MTX-TSL was evaluated using RM-1 prostate cancer cell inhibition assays. *In vivo* experiments were conducted on BDF1 mice inoculated with RM-1 cells to assess the tissue distribution and anticancer activity of MTX-TSL. Quality assessments of MTX-TSL revealed a pH of  $6.53 \pm 0.02$ , osmotic pressure of  $309 \pm 3$  mOsmol/Kg, particle size of  $100.10 \pm 1.50$  nm, and encapsulation efficiency of  $98.41\% \pm 0.23\%$ . Stability tests showed no major quality changes for liposome suspensions stored at  $2-8^\circ\text{C}$  for 2 months. *In vitro* release studies showed that MTX-TSL exhibited good thermosensitive properties. Experiments performed on BDF1 mice indicated that initiating hyperthermia before drug administration was beneficial for drug accumulation in tumor tissue and that MTX-TSL outperformed free drugs in suppressing tumor growth when combined with appropriate hyperthermia. MTX-TSL can effectively inhibit tumor growth while increasing the drug's therapeutic index.

**Keywords** Mitoxantrone, Thermosensitive liposome, Nanodelivery system, Thermosensitive properties, Antiproliferative activity against prostate cancer

Prostate cancer is one of the most common cancers in men worldwide, accounting for one of the highest incidences of malignant tumors in males<sup>1</sup>. Among men, this disease ranks second only to lung cancer in terms of cancer mortality. With the aging population and changes in lifestyle, its incidence is increasing. A major report on prostate cancer published in April 2024 by The Lancet (The Lancet Commission on prostate cancer: planning for the surge in cases)<sup>2</sup> predicted that the number of prostate cancer cases globally will rise from 1.4 million annually in 2020 to 2.9 million annually by 2040. The treatment options for prostate cancer include surgery, radiation and chemotherapy, hormone therapy, and immunotherapy<sup>3</sup>. With advancements in medical technology, these treatment modalities are constantly evolving and improving. Mitoxantrone (MTX)<sup>4</sup> is a cell cycle-nonspecific broad-spectrum anticancer drug with a chemical structure similar to doxorubicin (DOX) but without the amino sugar moiety at the C9 position; moreover, its anticancer activity is comparable to that of doxorubicin. MTX is primarily used to treat prostate cancer, acute nonlymphocytic leukemia, malignant lymphoma, and breast cancer, among other conditions. However, the use of MTX is associated with some serious adverse reactions, including potential cardiotoxicity during treatment<sup>5,6</sup>, which increases with cumulative dosage and may result in congestive heart failure months or years later. Furthermore, MTX can cause secondary acute myeloid leukemia (AML)<sup>7</sup> and bone marrow suppression<sup>8</sup>.

To improve the therapeutic index of MTX, many researchers have attempted to develop liposomal formulations of this drug<sup>9-11</sup>. Liposomes act as carriers for anticancer drugs and have excellent properties such as targeting, detoxification, and increased efficacy. They can aggregate in tumor areas to increase drug concentration via the enhanced permeation and retention effect<sup>12,13</sup>. MTX has two dissociable groups that allow it to form complex

<sup>1</sup>Department of Pharmacy, Hebei Medical University Third Hospital, No. 139 Ziqiang Road, Qiaoxi District, Shijiazhuang 050051, Hebei, China. <sup>2</sup>Department of Pharmacy, the Fourth Hospital of Hebei Medical University, Shijiazhuang 050011, China. <sup>3</sup>Hebei University of Chinese Medicine, No. 3 Xingyuan Road, Luquan District, Shijiazhuang 050091, Hebei, China. <sup>4</sup>These authors contributed equally: Yuan Gao and Tianjiao Wen. ✉email: tianwei@hebcm.edu.cn; congxinli@hebmu.edu.cn

aggregates with salts in the internal aqueous phase (such as sulfates, citrates, or phosphates), altering its release kinetics<sup>14</sup>. However, the challenge in developing MTX liposomes lies in effectively controlling drug release after they accumulate in tumor regions to achieve the desired therapeutic effect. Compared with conventional liposomes, thermosensitive liposomes have stronger tissue-targeting and controlled-release properties, which can increase the drug release rate<sup>15</sup>. Thermosensitive liposomes should be loaded with cell cycle-nonspecific broad-spectrum anticancer drugs; this way, when the drug is released in the tumor area, it can inhibit cancer cells at any stage of the cell cycle. Thermosensitive liposomes are a distinct class of triggerable liposomes. They are made of thermosensitive materials and frequently use phospholipids with a specific phase transition temperature to encapsulate the drug<sup>16</sup>. Following in vivo administration, these liposomes can be activated by local heating to rapidly release the encapsulated drug at the heated site, resulting in a targeted effect<sup>16</sup>. The use of thermosensitive liposomes for drug delivery, combined with localized heating at pathological sites, has emerged as a novel liposomal targeting strategy. An example of this is the thermosensitive liposomes formulation of doxorubicin, ThermoDox<sup>®</sup><sup>17,18</sup>, developed by Celision Corporation in collaboration with Duke University. This was the first thermosensitive liposome to undergo clinical trials. According to data analysis, in the subgroup of patients who received radiofrequency ablation for 45 min, ThermoDox<sup>®</sup> significantly improved progression-free survival and overall survival.

As a result, in the present study, the anticancer drug MTX was chosen as the model drug, and mitoxantrone thermosensitive liposome (MTX-TSL) were prepared based on the formulation of ThermoDox<sup>®</sup> to assess their efficacy against prostate cancer. Our findings indicated that using thermosensitive liposomes increased the release rate of MTX. The release behavior of MTX-TSL at different temperatures revealed that the drug release was very limited in a 37 °C water bath but increased considerably at 41 °C. Furthermore, prolonging the incubation duration at 41 °C substantially accelerated drug liberation, achieving cumulative release rates of approximately 80% within 30 min and 96% after 45 min. Taking advantage of the dual benefits of liposomes and hyperthermia, the targeting ability of liposomes was improved. This study systematically investigated the physicochemical properties of MTX-TSL, including their thermosensitivity and stability. Furthermore, their pharmacodynamics were assessed using a tumor-bearing mouse model, providing valuable insights for the development of new formulations.

## Methods

### Drugs and chemicals

MTX hydrochloride was purchased from Chongqing Kailin Co., Ltd (Chongqing, China). 1,2-distearoyl-sn-glycero-3-phosphoethanolamine-N-[methoxy(polyethyleneglycol)-2000] (DSPE-mPEG2000) and dipalmitoyl phosphatidylcholine (DPPC) were purchased from Lipoid GmbH (Germany). Mono-stearoyl phosphatidylcholine (MSPC) was purchased from Sigma-Aldrich corporation (America).

### Cell culture

RM-1 prostate cancer cells were obtained from the Shanghai Cell Bank of the Chinese Academy of Sciences (Shanghai, China). RM-1 cells were cultured in Roswell Park Memorial Institute 1640 (RPMI 1640) medium supplemented with 10% fetal bovine serum at 37 °C in a humidified atmosphere with 5% CO<sub>2</sub>. The cells were incubated until they were 80–90% confluent, then washed once with phosphate buffer saline (PBS), and digested with trypsin-ethylene diamine tetraacetic acid. The digestion was completed by adding a serum-containing medium and centrifuging the cells at 700 rpm for 5 min. The supernatant was discarded, and the collected cells were resuspended in a fresh culture medium before being seeded into new culture flasks. The cultures were then incubated in a Forma 3111 CO<sub>2</sub> incubator (Thermo Fisher Scientific, USA).

### Animal studies

Male BDF1 mice weighing approximately 20 g were purchased from Beijing Vital River Laboratory Animal Technology Co., Ltd (Beijing, China). Animal welfare and experimental procedures strictly adhered to the related ethics regulations of the Shijiazhuang Pharmaceutical Group Drug Research Institute. Mice were euthanized via isoflurane inhalation and subsequent cervical dislocation. The concentration of isoflurane was 2–2.5%, and anesthesia lasted approximately 5–8 min. The research was reported following the ARRIVE guidelines.

RM-1 cells were inoculated into the subcutaneous tissue of the hind limb of mice, with an inoculation volume of 0.05 mL containing approximately  $1.25 \times 10^5$  tumor cells. When the tumor volume reached a certain threshold, mice with consistent tumor growth were chosen and evenly distributed based on tumor volume. The dosing regimen was established as follows: using MTX as a reference, a single dose of 4 mg/kg was administered with a dosing volume of 20 mL/kg.

### Preparation of MTX-TSL

DPPC, MSPC, and DSPE-mPEG2000 were accurately weighed in a molar ratio of 90:10:4 and dissolved in chloroform in a round-bottom flask. The mixture was then subjected to rotary evaporation at 50 °C to obtain a thin film. The film was hydrated with a 0.3 mol/L pH 4.0 citrate buffer solution. Once the phospholipids were completely hydrated, a Liposofast-100 jacketed extruder (Avestin Inc.) equipped with a 0.08-μm filter membrane was used to extrude the liposomes, resulting in a uniform particle size distribution. The Sephadex G-75 gel column (2.5 × 10 cm) was packed and washed with three column volumes of a 20 mmol/L pH 7.6 histidine buffer solution. Blank liposomes were loaded onto the column, followed by additional washing to collect the eluent, which had a white milky appearance<sup>19</sup>. After dialysis, the drug loading capacity was calculated using a specific drug-to-lipid ratio. A 10-mg/mL mitoxantrone solution was added and incubated at 20–35 °C for the specified time. Following drug loading, the liposomes were subjected to secondary dialysis with a pH 6.5 solution containing 300 mmol/L sucrose and 20 mmol/L histidine. The resulting liposome injection was sterilized via

filtration, aliquoted, flushed with nitrogen, sealed, and stored at 2–8 °C. MTX liposome (MTX-L) was prepared in the absence of DPPC and MSPC using the same procedure as described above.

### Single-factor investigation of the formulation and process parameters for MTX-TSL

Using encapsulation efficiency (EE) as the primary evaluation index, we used a single-factor variation method to investigate the effects of four specific factors on liposome preparation: dialysis liquid composition, drug loading temperature, incubation time, and drug-to-lipid weight ratio.

In this study, we fixed other conditions and investigated how using 20 mmol/L histidine or 300 mmol/L sucrose containing 20 mmol/L histidine as the dialysis solution affected drug loading time and EE. The thermosensitive liposomes prepared in this study have a phase transition temperature of approximately 41 °C<sup>15</sup>. At the phase transition temperature, the permeability of the liposomal membrane significantly increases, whereas the stability of the liposomes decreases, resulting in the rapid collapse of the established pH gradient. Therefore, drug loading must be completed at lower temperatures. In this experiment, under fixed conditions, we changed the incubation temperature of the MTX solution with blank liposomes to 25 °C and 35 °C, respectively, to evaluate their effects on liposome formation and EE. In addition, we fixed other conditions while varying the incubation time of the MTX solution with blank liposomes to 5 min, 10 min, 20 min, 30 min, 45 min, and 60 min to investigate its effect on liposome formation and EE. The drug-to-lipid ratio has a significant impact on the encapsulation process: if the ratio is too high, the transmembrane pH gradient may be inadequate to accommodate all drugs; conversely, if the ratio is too low, less drug will be loaded into liposomes of equal weight, leading to low loading capacity. Given the high cost of liposome preparation, this may limit practical applications. As a result, we kept the loading conditions constant at 35 °C for 45 min and varied the drug-to-lipid ratio. We examined the loading amounts corresponding to 0.5 mg, 1 mg, and 1.5 mg of MTX per 10 mg of total phospholipid, achieving drug-to-lipid ratios of 1:20, 1:10, and 1:6.7, respectively, to determine the optimal drug-to-lipid ratio based on EE variations.

### Quality study of MTX-TSL

The quality of MTX-TSL was evaluated based on several parameters, including liposome appearance, pH, osmotic pressure, particle size and size distribution, zeta potential, EE, and drug content. In this study, the pH of MTX-TSL was determined using a DELTA 320 pH meter (Amettler Toledo, Switzerland). The osmotic pressure of MTX-TSL was measured using an SMC-30 osmometer (Tianjin Tianhe Instrument Co., Ltd., China). Particle size was determined using an S90 nanoparticle size analyzer (Malvern Instruments Ltd., UK). The zeta potential was determined using a dynamic lightscattering instrument (Zetasizer, Malvern, UK). To determine the drug content, 100 µL of MTX-TSL was placed in a 10-mL volumetric flask. Then, 20 µL of a 3% triton X-100 solution was added to disrupt the membrane, followed by the addition of purified water. The drug content was analyzed using high-performance liquid chromatography (HPLC) (Waters Corporation, USA) to determine the drug concentration.

The EE was calculated using the following formula:

$$EE (\%) = \frac{\text{The amount of MTX encapsulated in the liposomes}}{\text{The amount of MTX encapsulated in the liposomes} + \text{the amount of free MTX}} \times 100\%.$$

### Investigation of the thermosensitive properties of MTX-TSL

An ideal thermosensitive liposome should release drugs slowly at normal human body temperature. However, when heated at the target site, liposomes circulating in the blood that flow through or accumulate there can release a substantial amount of their contents, achieving the goal of targeted drug delivery. We investigated the thermosensitive properties of this formulation from two perspectives: fixed incubation times at different temperatures and varying incubation times at the phase transition temperature.

Study on the release of MTX-TSL at different temperatures: The liposomes were diluted in PBS to 0.1 mg/mL and then aliquoted into centrifuge tubes. These tubes were placed in a superheated circulating water bath at 37 °C, 38 °C, 39 °C, 40 °C, 41 °C, 42 °C, and 43 °C and incubated for 45 min. Immediately following incubation, the tubes were removed and placed in an ice bath to cool. A study on the release of MTX-TSL was also conducted in the presence of 50% serum. The EE of the liposomes was measured using dextran G-75 column chromatography. The release rate was computed as follows:  $\text{Release Rate (\%)} = (1 - \frac{\text{the content of the drug encapsulated by the liposome}}{\text{total drug content}}) \times 100\%$ .

Study on the release of MTX-TSL at phase transition temperature: The liposomes were diluted in PBS to 0.1 mg/mL and then aliquoted into centrifuge tubes. The centrifuge tubes were placed in a superconstant water bath circulator at 41 °C, and 1 mL was sampled at 5 min, 15 min, 30 min, 45 min, and 60 min. The collected samples were quickly placed in cold water. The release rate was then estimated.

### Investigation of the short-term stability of MTX-TSL

Liposome stability is influenced by factors such as liposome composition, particle size, physical and chemical properties of the loaded drug, external temperature, and environmental pH. Three batches of test samples were prepared using the optimal formulation and process and stored at 2–8 °C. The changes in appearance, particle size, zeta potential, pH, EE, release rate, and drug content were investigated at 1 day, 14 days, 1 month, and 2 months.

### Investigation of the tissue distribution of MTX-TSL

As described in Animal studies section, a prostate cancer model was established in mice. Once the tumor volume exceeded 100 mm<sup>3</sup>, the selected mice were randomly assigned to six groups, each consisting of four mice.

In groups 1 and 2 (pre-hyperthermia groups), the mice were anesthetized with 10% chloral hydrate, which was given at a dose of 3 mL/kg and induced anesthesia within 1 min. The tumor site was heated in a water bath for 15 min before injecting the drug through the tail vein. Following drug administration, group 1 was subjected to an additional 1 h of water bath heating at the tumor site, whereas group 2 resumed normal housing conditions. After an hour, the animals were euthanized to extract and separate the tumor and liver, which were then stored at  $-20^{\circ}\text{C}$  for later analysis. Group 1 was designated as the hyperthermia treatment group, and group 2 served as the control group.

In groups 3 and 4 (pre-injection-2 h groups), the mice received tail vein injections first. After 2 h of normal housing, they were anesthetized with 10% chloral hydrate. Group 3 was then subjected to an additional 1 h of water bath heating at the tumor site, whereas group 4 returned to normal housing conditions. An hour later, the animals were euthanized, and the tumor and liver were excised and stored at  $-20^{\circ}\text{C}$  for later analysis. Group 3 received heat treatment 2 h after injection, whereas group 4 served as the control group.

In groups 5 and 6 (pre-injection-4 h groups) mice received tail vein injections, followed by normal housing for 4 h before being anesthetized with 10% chloral hydrate. Group 5 was subjected to an additional 1 h of water bath heating at the tumor site, whereas group 6 was returned to normal housing conditions. After an hour, the animals were euthanized, and the tumor and liver were excised and stored at  $-20^{\circ}\text{C}$  for later analysis. Group 5 was identified as the hyperthermia treatment group administered 4 h post injection, whereas group 6 served as the control group.

Approximately 0.2 g of tissue was obtained, minced, and lysed with cell lysis buffer<sup>20</sup> (0.25 mol/L sucrose, 5 mmol/L Tris, 1 mmol/L  $\text{MgSO}_4$ , 1 mmol/L  $\text{CaCl}_2$ , pH 7.6) to prepare a tissue homogenate. Nuclei were extracted from the tumor tissue. The concentration of MTX in tissue samples and nuclear resuspension was determined using HPLC.

### Pharmacodynamics study of MTX-TSL

MTX-TSL growth inhibition assay at the cellular level: RM-1 cells were cultured under standard conditions, and logarithmic phase cells were collected. The cell suspension was adjusted to a density of 5000 cells per well before plating. MTX-TSL were diluted to 0.1 mg/mL in PBS buffer and subjected to various treatments: kept on ice, heated in a  $37^{\circ}\text{C}$  water bath for 45 min, heated in a  $41^{\circ}\text{C}$  water bath for 10 min, and heated in a  $41^{\circ}\text{C}$  water bath for 45 min. The treated liposomes were serially diluted and added to the cells, with 100  $\mu\text{L}$  per well, resulting in final concentrations of 60,000 ng/mL, 30,000 ng/mL, 15,000 ng/mL, 7500 ng/mL, 3750 ng/mL, 1725 ng/mL, 862.5 ng/mL, and 431.2 ng/mL after the addition of cells. The cells were incubated for 48 h, after which 20  $\mu\text{L}$  of MTT solution (5 mg/mL) was added to each well and the incubation was continued for an additional 4 h. Then, 150  $\mu\text{L}$  of DMSO was added to each well, and the plates were shaken carefully for 10 min. The optical density at 490 nm was measured with a microplate reader, and the IC<sub>50</sub> values were determined. The same method was used to calculate the IC<sub>50</sub> value of the untreated free drug.

Pharmacodynamics of MTX-TSL in tumor-bearing mice in vivo: The prostate cancer model in mice was established based on section “Animal studies”. Once the tumor volume exceeded 100 mm<sup>3</sup>, the mice were randomly divided into five groups based on tumor volume, with 10 mice in each group. The first group was given MTX-TSL combined with hyperthermia (MTX-TSL with prehyperthermia). The mice were first anesthetized with 10% chloral hydrate (3 mL/kg, inducing anesthesia in 1 min), and then the tumor area was heated in a water bath for 15 min. After heating, the mice were given a tail vein injection (the mice were still heated in the water bath during administration) and kept in the water bath for another hour before standard feeding. The second group received MTX-TSL along with posthyperthermia (MTX-TSL with posthyperthermia). The mice were given a tail vein injection, fed normally for 2 h, anesthetized with 10% chloral hydrate, and the tumor area was heated in a water bath for 1 h before standard feeding. The third group was given MTX-L, followed by normal feeding. The fourth group was given a free drug (MTX-free), followed by normal feeding. The fifth group served as the blank control group and received standard feeding. Throughout the experiment, the body temperature of the mice was monitored, and tumor growth was observed.

Evaluation indicators: (1) Tumor weight: After the experiment, tumors were excised and weighed. (2) Day 1 was designated as the time of the first administration; tumor length and width were measured every two days after treatment to calculate tumor volume and determine the average value, thereby plotting the tumor growth curve. The tumor volume was calculated using the following formula:  $V = 1/2 \times a \times b^2$ , where  $a$  and  $b$  are the tumor's length and width, respectively. (3) The relative tumor volume (RTV) was calculated using the following equation:  $\text{RTV} = V_t / V_0$ , where  $V_0$  is the tumor volume measured at the time of the first drug administration ( $d_0$ ), and  $V_t$  is the tumor volume measured at each subsequent time point. The RTV inhibition rate was calculated as  $(1 - T_{\text{RTV}} / C_{\text{RTV}}) \times 100\%$ , where  $T_{\text{RTV}}$  represents the RTV in the treatment group and  $C_{\text{RTV}}$  denotes the RTV in the negative control group.

### Statistical analysis

Statistical analysis was performed using GraphPad Prism (version 7.00, GraphPad Software) and SPSS version 24.0. Data are presented as mean  $\pm$  SD. For single comparisons, student's t-test was used when the data had a normal distribution with equal variance. For multiple comparisons, one-way ANOVA was used. A  $P$  value of  $<0.05$  was considered statistically significant.

## Results

### Preparation and quality evaluation of MTX-TSL

We conducted a screening of the formulation process of MTX-TSL using EE as the primary evaluation indicator. The final formulation was determined using a dialysis solution containing 20 mmol/L histidine, a drug loading temperature of  $35^{\circ}\text{C}$ , and a drug loading time of 45 min. The results showed that there was no statistically

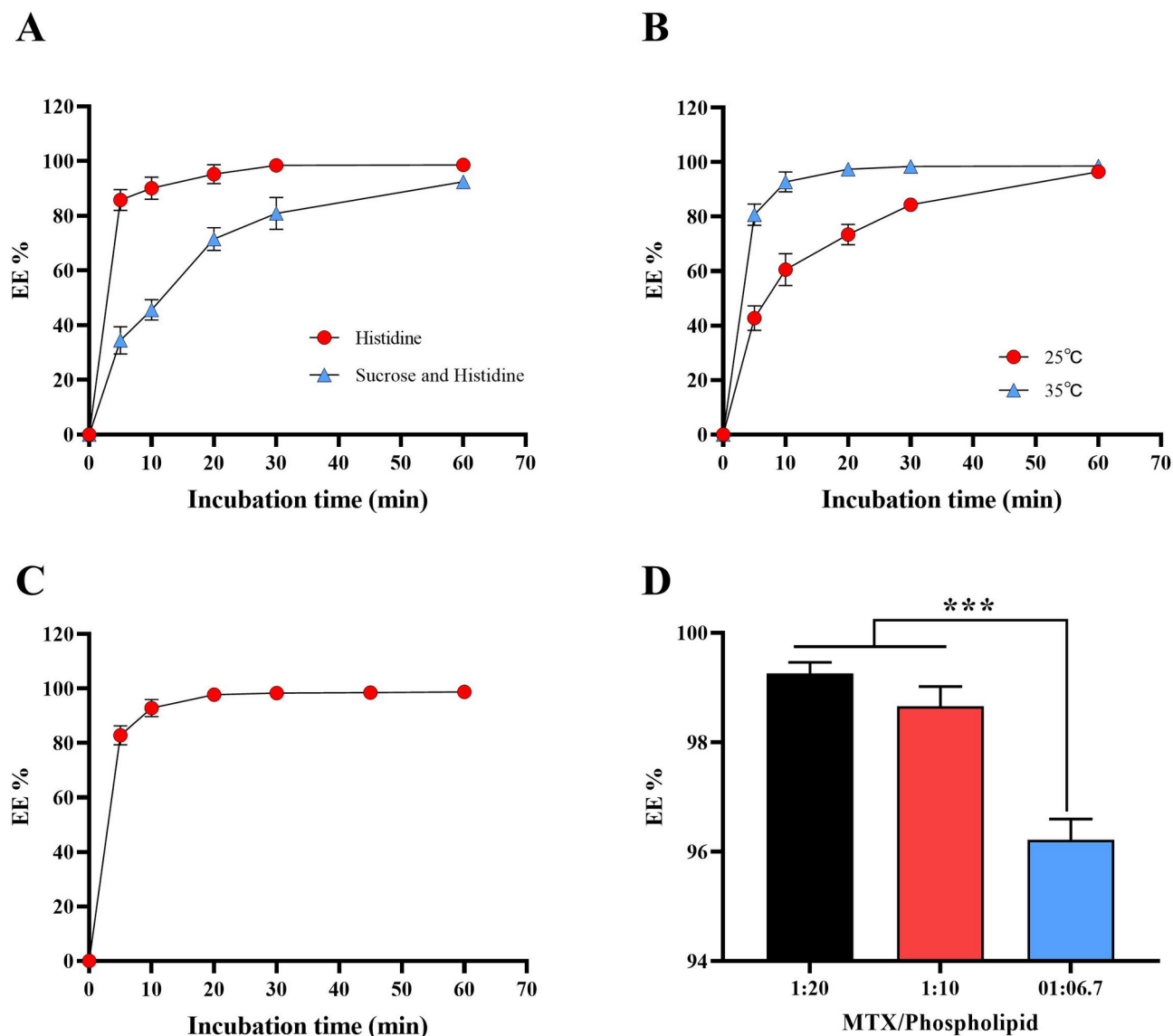


**Fig. 1.** Results of the single-factor investigation on the formulation process of MTX-TSL. (A) The effect of dialysis solution on the EE of MTX-TSL. (B) The effect of drug loading temperature on the EE of MTX-TSL. (C) The effect of drug loading time on the EE of MTX-TSL. (D) The effect of drug-to-lipid ratio on the EE of MTX-TSL. EE, encapsulation efficiency. \*\*\*  $P < 0.001$ .

Batch	Lipid composition (molar ratio)	Particle size (nm)	Zeta potential (mV)	pH	Osmotic pressure (mOsmol/Kg)	EE (%)	Drug content (mg/mL)
1	DPPC: MSPC: DSPE-mPEG2000 (90:10:4)	98.61	-34.52	6.52	309	98.66	1.10
2	DPPC: MSPC: DSPE-mPEG2000 (90:10:4)	101.60	-32.35	6.51	307	98.34	1.07
3	DPPC: MSPC: DSPE-mPEG2000 (90:10:4)	100.10	-33.66	6.55	312	98.22	1.03
Mean	DPPC: MSPC: DSPE-mPEG2000 (90:10:4)	100.10 ± 1.50	-33.51 ± 1.09	6.53 ± 0.02	309 ± 3	98.41 ± 0.23	1.07 ± 0.04

**Table 1.** Characterization of Mitoxantrone thermosensitive liposomes. EE encapsulation efficiency.

significant difference in EE between the drug-to-lipid ratios of 1:20 and 1:10 ( $P > 0.05$ ), but the EE decreased at a drug-to-lipid ratio of 1:6.7 ( $P < 0.05$ ). Based on the stability and practicality of the formulation, the optimal drug-to-lipid ratio was determined to be 1:10. The results are presented in Fig. 1.

We prepared three batches of MTX-TSL using the optimal process described above. The quality assessment results showed that MTX-TSL met the specifications for particle size, zeta potential, pH, osmotic pressure, EE, and content, as shown in Table 1. A study of their thermosensitive characteristics revealed that MTX-TSL



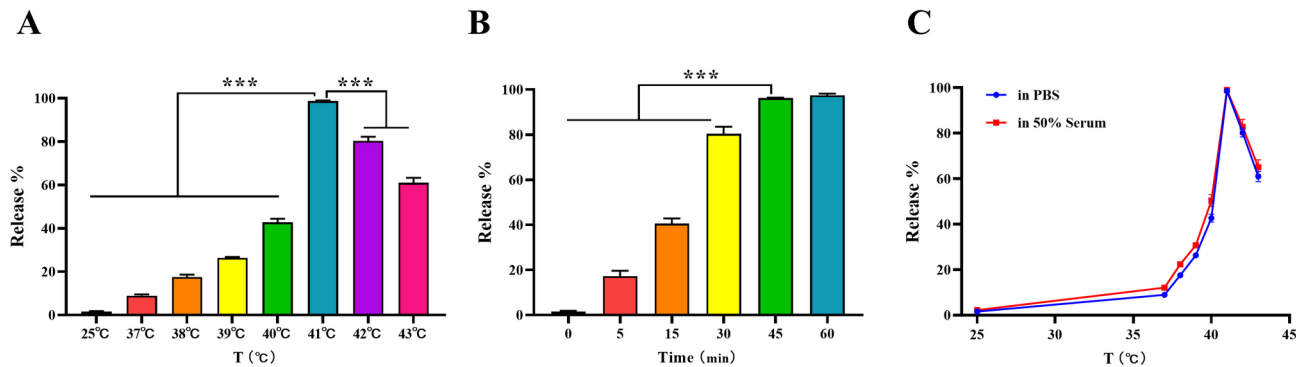


**Fig. 2.** Thermosensitive properties of MTX-TSL. (A) Release rate of MTX-TSL at different temperatures in PBS. (B) Release rate of MTX-TSL at the phase transition temperature in PBS. (C) Comparison between release of MTX-TSL in PBS and in 50% serum.\*\*\*  $P < 0.001$ .

Storage time	pH	Particle size	Content	EE (%)	Release rate (%)	
					(37 °C 1 h)	(41 °C 1 h)
1 day	6.52	98.25	1.10	98.66	6.3	89.23
	6.51	101.6	1.07	98.34	7.6	93.72
	6.55	98.5	1.03	98.22	8.2	95.06
14 days	6.46	101.4	1.12	98.59	7.5	92.4
	6.50	101	1.03	98.72	6.6	95.2
	6.51	100.1	1.02	98.36	8.9	97.07
1 month	6.43	100.5	1.09	98.62	6.5	40.3
	6.47	101.5	1.04	98.76	7.8	50.2
	6.46	98.9	1.01	98.91	7.6	26.95
2 months	6.43	98.25	1.05	99.02	8.5	9.89
	6.47	101.6	1.02	98.92	7.9	9.68
	6.46	98.5	0.99	98.79	6.7	15.74

**Table 2.** Results of long-term stability test. *EE* encapsulation efficiency.

released the drug over 1 h at various temperatures. The release test conducted in 50% serum showed similar release behavior as in PBS. Drug release rate was minimal at 37 °C, but it increased significantly at 41 °C ( $P < 0.05$ ). Furthermore, prolonging the incubation duration at 41 °C substantially accelerated drug liberation, achieving cumulative release rates of approximately 80% within 30 min and 96% after 45 min in PBS. There was no significant statistical difference in release rates between 45 min and 60 min ( $P > 0.05$ ), as shown in Fig. 2. The stability study revealed that MTX-TSL stored at 2–8 °C for 2 months showed no significant changes in EE, pH, particle size, and content. The results of each test item are presented in Table 2.

**Thermal therapy enhances the accumulation of liposomes at the tumor site**

We analyzed the effects of the timing of thermal therapy on the concentrations of MTX in the liver, tumor, and tumor cell nuclei. Our findings revealed that thermal therapy significantly increased drug accumulation within tumors while decreasing it in the liver, although the extent of variation differed among thermal therapy groups. In the group where thermal therapy was started before drug administration, the concentration of the drug in the tumor was over three times than that in the control group ( $P < 0.05$ ). In contrast, in groups where thermal therapy was started after drug administration 2–4 h, a smaller increase in drug accumulation in the tumor was observed ( $P > 0.05$ ). In the group where thermal therapy was started before administration, the drug concentration in the liver was significantly reduced ( $P < 0.05$ ), whereas in the groups where thermal therapy was started after administration 2–4 h, similar drug concentrations in the liver were observed ( $P > 0.05$ ). Furthermore, measurement of MTX concentrations in tumor cell nuclei confirmed the targeted action of thermal therapy. Given the strong binding affinity of MTX to cell nuclei, we extracted the nuclei from the tumor cells and measured the amount of MTX bound to them, which reflected the actual amount of MTX exerting its therapeutic effect. The concentration of MTX in the nuclei of the group where thermal therapy was started before drug administration was significantly higher than that in the other groups (Fig. 3).

To summarize, the use of thermal therapy facilitates drug accumulation at the tumor site. The extent of drug accumulation is related to the timing of thermal therapy; starting thermal therapy before drug administration and repeating it 1 h later is the most effective way to increase drug accumulation in the tumor.

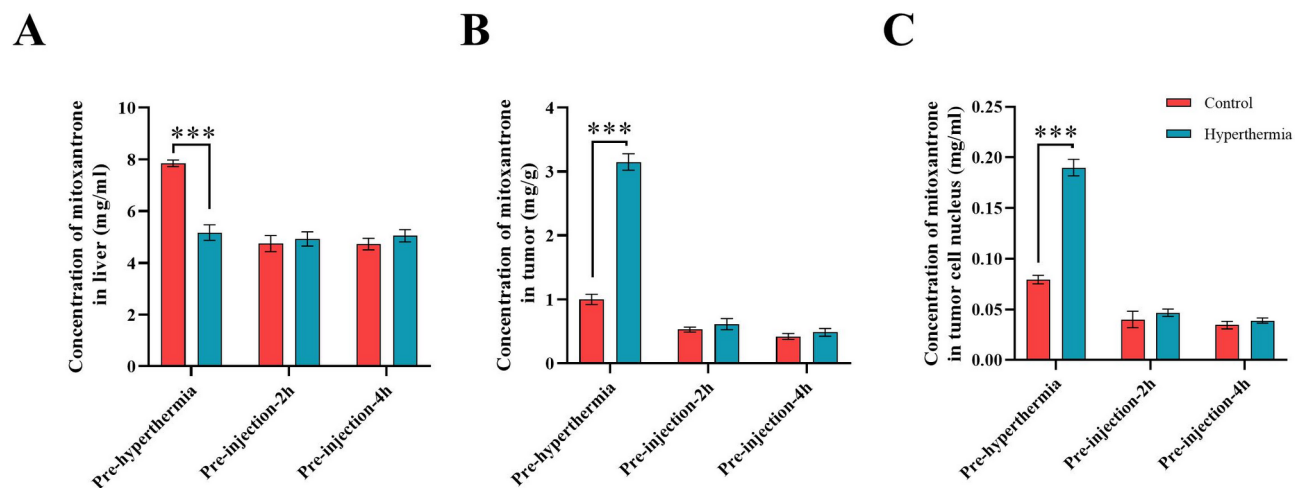


**Fig. 3.** Concentration of mitoxantrone in the liver (A), tumor (B), and tumor cell nucleus (C) of RM-1 bearing mice.\*\*\*  $P < 0.001$ .

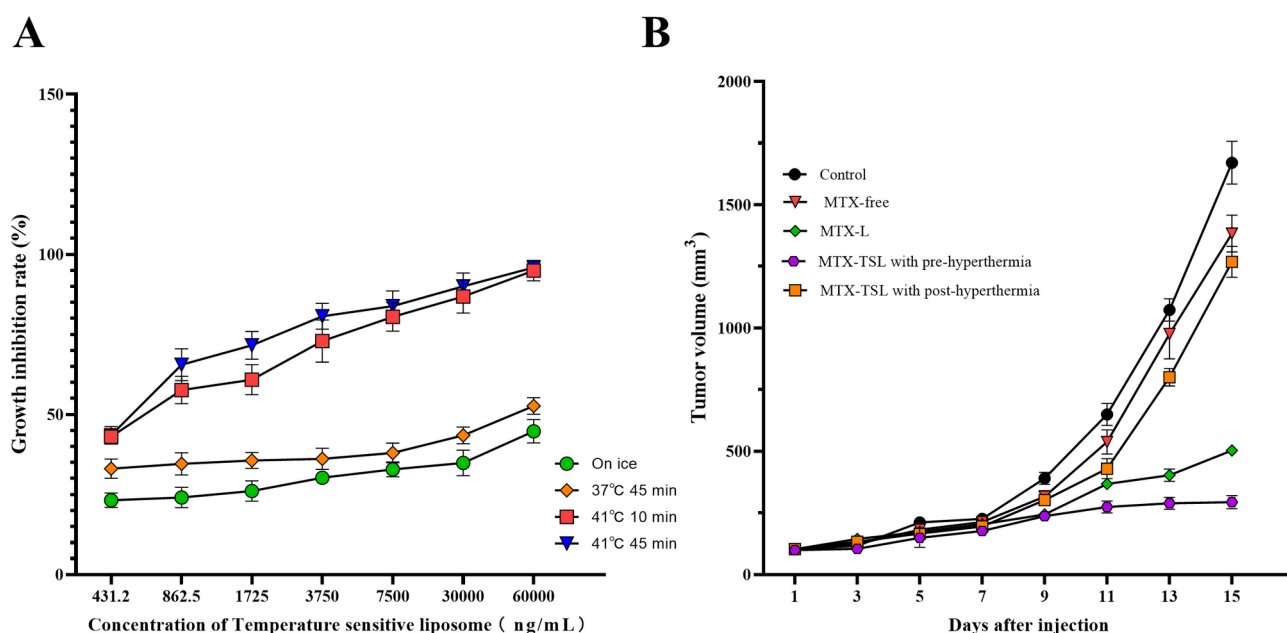


**Fig. 4.** MTX-TSL effectively enhances antitumor activity. (A) Cell growth inhibition curve. (B) Tumor growth curve after the administration of drugs.

### MTX-TSL effectively enhance antitumor activity

The results of the cell growth inhibition assay demonstrated that there was a small amount of free drug released from the liposomes when placed on ice or treated at 37 °C for 45 min, with significant variation compared with the 41 °C treatment groups. At 41 °C, the inhibition rates on RM-1 cells at 10 min and 45 min of treatment were comparable, with an IC<sub>50</sub> value of 783.3 ± 35 ng/mL at 10 min and an IC<sub>50</sub> value of 598.1 ± 71 ng/mL at 45 min. However, it is clear that the longer the treatment lasts, the more free drug is released, resulting in a stronger inhibitory effect on the cells, as shown in Fig. 4.

Following the completion of the pharmacodynamics experiment in tumor-bearing mice in vivo, the average tumor weight and inhibition rates were obtained, which are displayed in Table 3, and the tumor growth curves are illustrated in Fig. 4. According to the findings, tumor growth was inhibited in every treatment group. The group treated with MTX-TSL preheated for 15 min had slightly better results than the MTX-L group and significantly better results than the thermosensitive liposome group subjected to hyperthermia 2 h postadministration and the free drug group ( $P < 0.01$ ). Statistical analysis revealed significant differences among the 15-min preheated MTX-TSL, MTX-L, and blank groups ( $P < 0.01$ ) as well as between the 15-min preheated MTX-TSL, MTX-L

Treatment group	Tumor weight (g)	Inhibition rate (%)
MTX-TSL with prehyperthermia	0.235 ± 0.0263	86.1 **▲▲
MTX-TSL with posthyperthermia	1.098 ± 0.0682	34.8
MTX-L	0.405 ± 0.0321	76.0 **▲▲
MTX-free	1.216 ± 0.0516	27.9
Control	1.686 ± 0.0520	

**Table 3.** Weight and tumor Inhibition rate in different experimental groups of mice ( $\bar{x} \pm s.d.$ ,  $n = 10$ ). \* $P < 0.05$  and \*\* $P < 0.01$  compared with the control group; ▲ $P < 0.05$  and ▲▲ $P < 0.01$  compared with the MTX-free group.

and the free drug group ( $P < 0.01$ ). Significant differences were also observed between the two experimental groups of thermosensitive liposomes ( $P < 0.01$ ).

## Discussion

In this study, the liposomes were formulated using the liposomal phospholipid composition of ThermoDox<sup>®</sup> (DPPC: DSPC: DSPE-mPEG2000 = 90:10:4, molar ratio)<sup>21</sup>. Using the film hydration method described in a previous study<sup>19</sup>, we optimized the liposome preparation process using EE as the evaluation indicator. We investigated the effects of various dialysis solutions, incubation temperatures, incubation times, and drug-to-phospholipid weight ratios on the liposomes using single-factor experiments, eventually determining the formulation process for MTX-TSL. As normal human tissues cannot tolerate temperatures above 45 °C and the phase transition temperature of DPPC is 41.5 °C<sup>22</sup>, which is slightly higher than the normal human body temperature, DPPC is the preferred membrane material for thermosensitive liposomes. Hemolytic phospholipids can severely disrupt the lipid bilayer<sup>23</sup>, and even low concentrations can significantly increase liposomal membrane permeability. As a result, incorporating MSPC into the lipid bilayer improves drug release at phase transition temperatures. Above all, we developed and improved the formulation and preparation process for MTX-TSL.

The effect of dialysis solution on the drug loading of thermosensitive liposomes is an important finding in this study. When the weakly basic drug MTX hydrochloride was incubated with blank liposomes following dialysis, the electrically neutral MTX rapidly diffused across the membrane into the aqueous phase of the liposomes, where it was quickly protonated and formed a stable complex with citrate ions. During the experiments, we observed that the presence or absence of sucrose in the external phase had a significant influence on the rate and extent of drug loading. We investigated this phenomenon and found that using a 20 mmol/L histidine solution as the dialysis solution increased the drug loading amount and loading rate of the liposomes compared with using a 300 mmol/L sucrose and 20 mmol/L histidine solution as the dialysis solution. This result can be attributed to the difference in osmotic pressure between the external phase of the liposomes. The outer solution of liposomes dialyzed with 20 mmol/L histidine is hypotonic compared with the inner aqueous phase, allowing water molecules to enter the internal aqueous phase via the lipid bilayer. This increases the volume of the internal aqueous phase and the distance between phospholipid molecules in the liposomal membrane, improving membrane permeability. As a result, MTX can pass more easily through the lipid bilayer and into the internal aqueous phase, increasing the drug loading rate. Following the drug loading phase, liposomes were subjected to secondary dialysis with a pH 6.5 solution containing 300 mmol/L sucrose and 20 mmol/L histidine. The secondary dialysis was performed to improve the storage stability of the liposomes, as phospholipids have the lowest hydrolysis rate at pH 6.5<sup>24,25</sup>. The addition of 300 mmol/L sucrose to the secondary dialysis served two purposes: it adjusted the osmotic pressure of the external phase of the liposomes and acted as a cryoprotectant, allowing the liposomes to be stored under frozen conditions<sup>26</sup>.

In recent years, several research groups have developed novel formulations of mitoxantrone liposomes. Estrone-targeted liposomes for MTX can effectively enter and accumulate in tumor cells that express estrogen receptors, thereby extending the circulation time in vivo<sup>27</sup>. Folate-targeted liposomes, which load folate onto their surface, can improve MTX accumulation in tumor cells with high folate receptor expression<sup>10</sup>. MTX-loaded pH-sensitive fusogenic liposomes are more cytotoxic in human breast cancer cell line (MCF-7) and human prostate cancer cell line (PC-3) than control liposomes<sup>28</sup>. Most studies have focused on the targeting capabilities of mitoxantrone liposomes; however, triggering liposome release in tumor tissues and increasing the drug release rate at the tumor site remain significant challenges in current liposome research. The development of thermosensitive liposomes could provide a solution to these technical challenges. Several preclinical studies have supported the relationship between heating and chemotherapy efficacy. For example, Alawak M and colleagues incorporated gadolinium into doxorubicin liposomes and used hyperthermia to promote drug release in targeted tissues, thereby improving the anticancer effect of doxorubicin against triple-negative breast cancer<sup>29</sup>. Another study by Cao X demonstrated that bisdemethoxycurcumin thermosensitive liposomes released the drug quickly during localized hyperthermia (42 °C) and induced cell apoptosis in a short time<sup>30</sup>. Currently, there are no reports indicating that MTX-TSL have antiprostata cancer activity. We intend to use thermosensitive materials as membrane components to formulate thermosensitive liposomes. Following in vivo administration, we used localized heating to activate drug release from liposomes in the tumor region, increasing their targeting and anticancer activities.



ThermoDox<sup>®</sup>, the first thermosensitive liposome to enter clinical trials, was tested in a randomized, double-blind phase III clinical trial that compared the efficacy of ThermoDox<sup>®</sup> combined with radiofrequency ablation with that of radiofrequency ablation alone in the treatment of inoperable hepatocellular carcinoma. Although the clinical outcomes failed to meet the primary expected endpoint, additional data analysis conducted by Celsion Corporation indicated that in the subgroup receiving radiofrequency ablation for 45 min or more, ThermoDox<sup>®</sup> greatly enhanced progression-free survival and overall survival<sup>17</sup>. This finding suggests that the combination strategy of liposomal drug delivery and hyperthermia may impact treatment efficacy. Research by G. Kong et al. demonstrated that hyperthermia can increase the pore size between tumor microvascular endothelial cells, facilitating increased extravasation into the tumor interstitium<sup>31</sup>. This study focused on examining the impact of the timing of hyperthermia on the efficacy of MTX-TSL. In vitro thermosensitivity experiments indicated that the optimal temperature and duration for hyperthermia for the prepared MTX-TSL were 41 °C and 45 min, respectively, providing a practical basis for subsequent in vivo experiments. To examine the effect of hyperthermia timing on drug distribution in vivo, we designed three treatment regimens: initiating hyperthermia before drug administration, administering hyperthermia 2 h post injection, and administering hyperthermia 4 h post injection. The findings revealed that initiating hyperthermia before drug administration increased blood perfusion in the tumor region, allowing for greater liposome accumulation in the tumor area and effective drug release via hyperthermia. Compared with the control group, the drug concentration in the tumor increased, whereas the drug concentration in the liver decreased. In contrast, the groups that received hyperthermia 2 h and 4 h after administration showed a lower increase in drug concentration at the tumor site than the control group, indicating that posthyperthermia had no significant effect on drug accumulation in the tumor. This could be attributed to the unique properties of thermosensitive liposomes, which facilitate rapid drug release and have a short half-life<sup>19</sup>. Thus, drug distribution occurs relatively quickly, primarily in organs with high blood flow, such as the liver. As a result, when hyperthermia was administered 2–4 h later, the drug distribution was nearly complete. Subsequent efficacy experiments investigated the effect of hyperthermia on therapeutic effects, revealing that the initiating hyperthermia group had a great advantage in inhibiting tumor growth compared with both the posthyperthermia and control groups, indicating good anticancer activity against prostate cancer.

## Conclusion

This study uses MTX, an antitumor drug, as a model drug and thermosensitive liposomes as drug carriers, providing a new drug delivery system for the treatment of prostate cancer. The preparation process for these liposomes is simple, resulting in high encapsulation efficiency, good reproducibility, and significant thermosensitivity. When combined with hyperthermia, this system significantly improves the targeting capability of liposomes, effectively suppresses tumor growth, and increases the therapeutic index of the drug. This study provides methodological guidance and experimental foundations for the development of MTX-TSL, emphasizing their potential clinical translational value and laying a strong foundation for prostate cancer research and treatment.

## Data availability

All data used for the analyses in this report are available from the corresponding author on reasonable request.

Received: 4 February 2025; Accepted: 30 April 2025

Published online: 07 May 2025

## References

- Gandaglia, G. et al. Epidemiology and prevention of prostate Cancer. *Eur. Urol. Oncol.* **4** (6), 877–892. <https://doi.org/10.1016/j.eur.2021.09.006> (2021).
- James, N. D. et al. The lancet commission on prostate cancer: planning for the surge in cases. *Lancet* **403** (10437), 1683–1722. [https://doi.org/10.1016/S0140-6736\(24\)00651-2](https://doi.org/10.1016/S0140-6736(24)00651-2) (2024).
- Sekhoacha, M. et al. Prostate Cancer review: genetics, diagnosis, treatment options, and alternative approaches. *Molecules* **27** (17), 5730. <https://doi.org/10.3390/molecules27175730> (2022).
- Evison, B. J., Sleebs, B. E., Watson, K. G., Phillips, D. R. & Cutts, S. M. Mitoxantrone, more than just another topoisomerase II poison. *Med. Res. Rev.* **36** (2), 248–299. <https://doi.org/10.1002/med.21364> (2016).
- Kim, C. W. & Choi, K. C. Effects of anticancer drugs on the cardiac mitochondrial toxicity and their underlying mechanisms for novel cardiac protective strategies. *Life Sci.* **277**, 119607. <https://doi.org/10.1016/j.lfs.2021.119607> (2021).
- Kouwenberg, T. W. et al. Acute and early-onset cardiotoxicity in children and adolescents with cancer: a systematic review. *BMC Cancer*. **23** (1), 866. <https://doi.org/10.1186/s12885-023-11353-9> (2023).
- Joannides, M. et al. Molecular pathogenesis of secondary acute promyelocytic leukemia. *Mediterr. J. Hematol. Infect. Dis.* **3** (1), e2011045. <https://doi.org/10.4084/MJHID.2011.045> (2011).
- Seiter, K. Toxicity of the topoisomerase II inhibitors. *Expert Opin. Drug Saf.* **4** (2), 219–234. <https://doi.org/10.1517/14740338.4.2.219> (2005).
- Jing, L. et al. Targeted delivery strategy of indocyanine green-mitoxantrone loaded liposomes co-modified with BTP-7 and BR2 for the treatment of glioma. *Pharm. Dev. Technol.* **8**, 1–11. <https://doi.org/10.1080/10837450.2024.2448619> (2025).
- Wen, T. et al. Evaluation of new folate Receptor-mediated Mitoxantrone targeting liposomes in vitro. *Curr. Pharm. Biotechnol.* **25** (4), 510–519. <https://doi.org/10.2174/0113892010258845231101091359> (2024).
- Amer Ridha, A. et al. A promising dual-drug targeted delivery system in cancer therapy: nanocomplexes of folate-apoferritin-conjugated cationic solid lipid nanoparticles. *Pharm. Dev. Technol.* **26** (6), 673–681. <https://doi.org/10.1080/10837450.2021.1920037> (2021).
- Wong, A. D., Ye, M., Ulmschneider, M. B. & Searson, P. C. Quantitative analysis of the enhanced permeation and retention (EPR) effect. *PLoS One*. **4** (5), e0123461. <https://doi.org/10.1371/journal.pone.0123461> (2015).
- Golombek, S. K. et al. Tumor targeting via EPR: strategies to enhance patient responses. *Adv. Drug Deliv. Rev.* **130**, 17–38. <https://doi.org/10.1016/j.addr.2018.07.007> (2018).
- Li, C. et al. Encapsulation of Mitoxantrone into pegylated suvs enhances its antineoplastic efficacy. *Eur. J. Pharm. Biopharm.* **70** (2), 657–665. <https://doi.org/10.1016/j.ejpb.2008.05.019> (2008).

15. Chaudhry, M., Lyon, P., Coussios, C. & Carlisle, R. Thermosensitive liposomes: a promising step toward localised chemotherapy. *Expert Opin. Drug Deliv.* **19** (8), 899–912. <https://doi.org/10.1080/17425247.2022.2099834> (2022).
16. Abuwatfa, W. H., Awad, N. S., Pitt, W. G. & Hussein, G. A. Thermosensitive polymers and Thermo-Responsive liposomal drug delivery systems. *Polym. (Basel)*. **14** (5), 925. <https://doi.org/10.3390/polym14050925> (2022).
17. Borys, N. & Dewhirst, M. W. Drug development of lyso-thermosensitive liposomal doxorubicin: combining hyperthermia and thermosensitive drug delivery. *Adv. Drug Deliv. Rev.* **178**, 113985. <https://doi.org/10.1016/j.addr.2021.113985> (2021).
18. Regenold, M. et al. Turning down the heat: the case for mild hyperthermia and thermosensitive liposomes. *Nanomedicine* **40**, 102484. <https://doi.org/10.1016/j.nano.2021.102484> (2022).
19. Tian, W. et al. Repeated injection of Mitoxantrone containing thermosensitive liposomes in rat induced ABC phenomenon. *Yao Xue Xue Bao*. **49** (2), 256–259 (2014). Chinese.
20. Dams, E. T. et al. Accelerated blood clearance and altered biodistribution of repeated injections of sterically stabilized liposomes. *J. Pharmacol. Exp. Ther.* **292**, 1071–1079 (2000).
21. Chang, H. I. & Yeh, M. K. Clinical development of liposome-based drugs: formulation, characterization, and therapeutic efficacy. *Int. J. Nanomed.* **7**, 49–60. <https://doi.org/10.2147/IJN.S26766> (2012).
22. Mishra, S., Mishra, A. K. & Sharma, R. Structural dynamics of chlorpromazine (CPZ) drug with dipalmitoylphosphatidylcholine (DPPC) lipid: a potential drug for SARS-CoV-2. *J. Biomol. Struct. Dyn.* **41** (16), 7595–7602. <https://doi.org/10.1080/07391102.2022.2123393> (2023).
23. Inoue, K. & Kitagawa, T. Effect of exogenous lysolecithin on liposomal membranes. Its relation to membrane fluidity. *Biochim. Biophys. Acta*. **363** (3), 361–372. [https://doi.org/10.1016/0005-2736\(74\)90075-3](https://doi.org/10.1016/0005-2736(74)90075-3) (1974).
24. Kirpotin, D. B. et al. Drug stability and minimized Acid-/Drug-Catalyzed phospholipid degradation in liposomal Irinotecan. *J. Pharm. Sci.* **112** (2), 416–434. <https://doi.org/10.1016/j.xphs.2022.11.025> (2023).
25. Wang, C., Gamage, P. L., Jiang, W. & Mudalige, T. Excipient-related impurities in liposome drug products. *Int. J. Pharm.* **657**, 124164. <https://doi.org/10.1016/j.ijpharm.2024.124164> (2024).
26. Gala, R. P., Khan, I., Elhissi, A. M. & Alhnan, M. A. A comprehensive production method of self-cryoprotected nano-liposome powders. *Int. J. Pharm.* **486** (1–2), 153–158. <https://doi.org/10.1016/j.ijpharm.2015.03.038> (2015).
27. Xu, G. et al. Estrone-targeted liposomes for Mitoxantrone delivery via Estrogen receptor: in vivo targeting efficacy, antitumor activity, acute toxicity and pharmacokinetics. *Eur. J. Pharm. Sci.* **161**, 105780. <https://doi.org/10.1016/j.ejps.2021.105780> (2021).
28. Ghanbarzadeh, S., Arami, S., Pourmoazzen, Z., Ghasemian-Yadegari, J. & Khorrami, A. Plasma stable, pH-sensitive fusogenic polymer-modified liposomes: A promising carrier for Mitoxantrone. *J. Biomater. Appl.* **29** (1), 81–92. <https://doi.org/10.1177/0885328213515288> (2014).
29. Alawak, M. et al. Magnetic thermosensitive liposomes loaded with doxorubicin. *Methods Mol. Biol.* **2622**, 103–119. [https://doi.org/10.1007/978-1-0716-2954-3\\_9](https://doi.org/10.1007/978-1-0716-2954-3_9) (2023).
30. Cao, X. et al. Microfluidic fabricated bisdemethoxycurcumin thermosensitive liposome with enhanced antitumor effect. *Int. J. Pharm.* **641**, 123039. <https://doi.org/10.1016/j.ijpharm.2023.123039> (2023).
31. Kong, G., Braun, R. & Dewhirst, M. W. Characterisation of the effect of hyperthermia on nanoparticle extravasation from tumor vasculature. *Cancer Res.* 3027–3032. (2001).

## Acknowledgements

We appreciate the support of Professor Chunlei Li in this study.

## Author contributions

Congxin Li and Wei Tian conceptualized and designed the project. Bin Shan, Meng Meng and Jing Bai performed the experiments and interpreted the results. Yuan Gao, Wei Tian and Congxin Li analyzed the data. Yuan Gao, Tianjiao Wen and Congxin Li wrote the manuscript. Congxin Li edited the manuscript. Congxin Li and Wei Tian supervised the project. All authors have read and agreed to the published version of the manuscript.

## Funding

This work was supported by the Medical Science Research Project of Hebei(20250112) and Natural Science Foundation of Hebei Province (H2024206062).

## Declarations

## Competing interests

The authors declare no competing interests.

## Institutional review board statement

Animal experiments in this study were approved by the animal ethics committees of Shijiazhuang Pharmaceutical Group Drug Research Institute, with the approval number: 20240783. All animal experiments were performed in accordance with the international, national, and institutional guidelines for animal care.

## Additional information

**Correspondence** and requests for materials should be addressed to W.T. or C.L.

**Reprints and permissions information** is available at [www.nature.com/reprints](http://www.nature.com/reprints).

**Publisher's note** Springer Nature remains neutral with regard to jurisdictional claims in published maps and institutional affiliations.

**Open Access** This article is licensed under a Creative Commons Attribution-NonCommercial-NoDerivatives 4.0 International License, which permits any non-commercial use, sharing, distribution and reproduction in any medium or format, as long as you give appropriate credit to the original author(s) and the source, provide a link to the Creative Commons licence, and indicate if you modified the licensed material. You do not have permission under this licence to share adapted material derived from this article or parts of it. The images or other third party material in this article are included in the article's Creative Commons licence, unless indicated otherwise in a credit line to the material. If material is not included in the article's Creative Commons licence and your intended use is not permitted by statutory regulation or exceeds the permitted use, you will need to obtain permission directly from the copyright holder. To view a copy of this licence, visit <http://creativecommons.org/licenses/by-nc-nd/4.0/>.

© The Author(s) 2025